

Small-q phonon mediated singlet and chiral spin triplet superconductivity in LiFeAs

A. Aperis* and G. Varelogiannis†

Department of Physics, National Technical University of Athens, GR-15780 Athens, Greece

We report fully momentum dependent, self-consistent calculations of the gap symmetry, Fermi surface (FS) anisotropy and T_c of superconducting (SC) LiFeAs using the experimental band structure and a realistic small-q electron phonon interaction within the framework of Migdal-Eliashberg theory. In the stoichiometric regime, we find the exact s_{++} gap as reported by ARPES. For slight deviations from stoichiometry towards electron doping, we find that a *chiral triplet* $p_x + ip_y$ state stabilizes near T_c and that at lower temperatures a *transition from the triplet to singlet* s_{\pm} SC takes place. Further doping stabilizes the chiral p-wave SC down to $T=0$. Precisely the same behavior was observed recently by NMR. Our results provide a natural and universal understanding of the conflicting experimental observations in LiFeAs.

PACS numbers: 74.20.-z, 74.20.Rp, 74.70.Xa

In iron arsenide superconductors are observed not only the higher critical temperatures after those observed in cuprates but also a plethora of exciting phenomena yet to be understood. Perhaps the most challenging compound is the stoichiometric LiFeAs [1] which exhibits a surprisingly exotic superconducting phenomenology. Measurements of NMR [2], inelastic neutron scattering [3] and specific heat [4] in this compound have been interpreted in terms of multigap singlet s_{\pm} SC [5]. However, the gap seen by ARPES indicates an anisotropic, singlet and one sign s_{++} order parameter [6, 7]. On the other hand, there is also consistent evidence for *p-wave spin triplet SC* in LiFeAs, first reported by quasiparticle interference (QPI) [8] and NMR [9]. Subsequent high magnetic field measurements have found that this state can also be induced by the field and it is *chiral* [10].

The NMR data have posed yet another extraordinary puzzle. Depending on small changes of the stoichiometry, some of the samples exhibit singlet SC, while the slightly more electron doped samples show triplet SC [9]. Moreover, it was recently reported that some samples exhibit a *temperature induced singlet to triplet transition* as temperature rises [11]. Clearly, not only do we observe in LiFeAs the highest temperature, by an order of magnitude, *triplet* SC state ($T_c=16-18$ K), but in addition this state emerges away from any magnetically ordered phase and exhibits some of the most surprising phase transition phenomena in a SC regime. Therefore, understanding theoretically the complex and seemingly conflicting SC phenomenology of LiFeAs is arguably one of the most challenging issues in the field of superconductivity.

The electronic structure of LiFeAs is characterized by reduced nesting properties and a *Van Hove* point (VHp) at the *center* of the Brillouin Zone (BZ) [12] (see Fig.1(a)). Although antiferromagnetic spin fluctuations (SFs) are generally weak in this material [2, 6, 13], their importance for SC is yet unresolved [14]. On the contrary, there is clear evidence of an enhanced electron-phonon interaction (EPI), strong enough to account for lifetime effects and the order of magnitude of the mea-

sured T_c [15]. So far, it has been argued that ferromagnetic SFs may drive the triplet SC [16]. On the other hand, the s_{++} SC has been interpreted in terms of orbital fluctuations assisted by phonons [17]. Even if either mechanism is proven relevant for LiFeAs, it still remains unclear how it could explain coherently the conflicting gap symmetry observations.

In this Letter we demonstrate that *all* of the aforementioned exotic phenomenology is consistently explained, in a unified way, if the enhanced EPI in this material has a momentum dependence peaked at *small-q*, similar to the one observed recently in cuprates [18]. Our analysis is based on fully anisotropic, self-consistent calculations of the SC gap within the Eliashberg approach, assuming a realistic small-q EPI and using the ARPES resolved multi-band structure for LiFeAs as reported by the experiments. Remarkably, using an overall electron-phonon coupling (EPC) strength of $\lambda = 1.38$ consistent with phonon damping effects in the ARPES spectra and reasonable characteristic phonon frequencies of about 100 K, the same Eliashberg calculations produce the right critical temperatures as well.

Small-q EPI can occur due to strong ionic and/or Coulombic effects [19–27]. Note that large ionic polarizabilities that may lead to enhanced dielectricity have indeed been reported in pnictides [28, 29]. It was early on understood that small-q EPI may lead to *unconventional* SC of d-wave type in the cuprates [25] and recent findings support the relevance of this type of interaction in these materials [18, 27]. Other unconventional SC materials, including κ -BEDT organic salts [30], the heavy fermion UPd₂Al₃ [31] and cobaltites [32] have also been shown within a BCS framework to be compatible with this generic picture. Recently, the first multiband BCS approach with the small-q EPI mechanism in pnictides [33] established that the reported unconventional SC states are compatible with the measures of finite isotope effect [34]. Our present fully momentum dependent Eliashberg calculations specifically dedicated to LiFeAs are of unprecedented precision. The quality with which

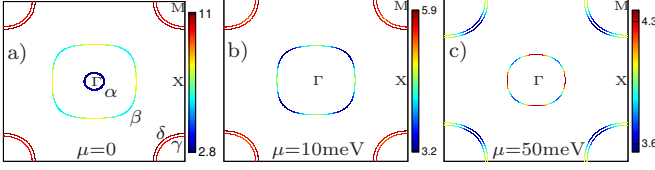


FIG. 1. (Color online) (a)-(c) The FS of LiFeAs colored by velocity for $\mu=[0, 10, 50]$ meV. The α pocket is very shallow and possesses high and isotropic DOS. The remaining FS pockets, exhibit DOS maxima along Γ -M that are enhanced by doping.

the experimental behavior of LiFeAs is reproduced as well as the fact that a *chiral triplet* SC state in a real material is plausibly associated with a *phononic* mechanism, has broad implications for the whole field of unconventional superconductivity.

We parametrize the EPC as an effective, yet realistic, kernel separable over momentum and Matsubara frequency: $\lambda(\mathbf{k}, \mathbf{k}'; n, n') = \lambda_{\mathbf{k}\mathbf{k}'} \lambda_{nn'}$, where $\lambda_{nn'}$ has an Einstein form and $\lambda_{\mathbf{k}\mathbf{k}'} = \frac{N_0 V_{ph}}{q_c^2 + |\mathbf{k} - \mathbf{k}'|^2}$, with V_{ph} an effective potential and N_0 the DOS on the FS. The momentum cutoff q_c selects the small wave vectors in the attractive phonon part while at larger wave vectors the repulsive Coulomb pseudopotential may prevail. For example, such a cutoff may arise naturally due to the interplay between enhanced dielectricity and the long range nature of the Coulomb potential. The simplest approximation to this case maps q_c to the Thomas-Fermi (TF) screening wavevector, $q_{TF} \propto \sqrt{N_0/\epsilon}$ where ϵ is the dielectric constant [18, 20, 21]. In the case of LiFeAs, this provides with the rough estimate that q_c should decrease away from stoichiometry, i.e. from the VHp. A small q_c leads to a *momentum decoupling* (MD) situation [24]. In the MD regime the gap function loses its rigidity in momentum space and becomes correlated with the variations of the DOS, leading to FS momentum dependent and possibly unconventional SC. For a multiband system, this also leads to the dominance of the EPI for intraband channels, while the Coulomb pseudopotential provides a repulsive interband coupling, allowing for a sign alternating SC gap [33]. Since by definition: $\lambda = \langle \lambda(\mathbf{k}, \mathbf{k}'; 0) \rangle_{\mathbf{k}, \mathbf{k}'}^{FS}$, in the following we fix λ to the experimentally reported value [15] by adjusting V_{ph} , so that for each value of q_c , $\lambda = \langle \lambda_{\mathbf{k}, \mathbf{k}'} \rangle_{\mathbf{k}, \mathbf{k}'}^{FS} = 1.38$, where $\langle \dots \rangle_{\mathbf{k}}^{FS}$ is a FS average.

For the band structure of LiFeAs we use a four band Tight-Binding (TB) model elaborated by the IFW group as a fit to ARPES data [14, 35]. Hence our realistic input, captures the experimentally resolved FS of LiFeAs extremely well (Fig.1(a)). We model the effect of doping in the rigid band approximation by subtracting a chemical potential, μ , from all four bands. For $\mu > 0$ ($\mu < 0$) the system is electron (hole) doped. We refer to the inner hole, outer hole, inner electron and outer electron pocket as α, β, γ and δ , respectively. In Fig.1(a)-(c) the FS of this model is shown, colored by velocity at different val-

ues of μ . The presence of a VHp at Γ is evident by the blue color denoting a very high and isotropic DOS over α . This pocket is very shallow thus, a slight deviation from stoichiometry, which translates to $\mu > 5.2$ meV, is enough to remove it from the FS as shown in Fig1(b)-(c). The remaining pockets exhibit some anisotropy, which is enhanced with doping, and maximum DOS along Γ -M.

Having analyzed the input of our theory, we now discuss briefly (for details see the SOM) the technique that we employ to obtain our results. Our starting point is the fully anisotropic Eliashberg equations (e.g. see ref.[36]). The EPC that we use implies that the SC gap function is also separable and can be written as: $\Delta_{\mathbf{k}, n} = \Delta_n g_{\mathbf{k}}$, where Δ_n is the gap amplitude distributed over the Matsubara frequencies and $g_{\mathbf{k}}$ contains the momentum dependence of the SC gap ($|g_{\mathbf{k}}| \leq 1$). Utilizing this property, we end up with two eigenvalue equations at $T=T_c$ instead of one, as in standard Eliashberg theory. The first one is the usual eigenvalue problem but extended to account for the full anisotropy of the gap:

$$\sum_{n'=0}^N \left[a \cdot (\lambda(n - n') + \lambda(n + n' + 1)) - 2b - c \cdot \delta_{nn'} \right. \\ \left. \times \left(\lambda(0) + 2 \sum_{m=1}^n \lambda(m) \right) - \frac{\delta_{nn'} |\omega_{n'}|}{\pi T_c} \right] \tilde{\Delta}_{n'} = 0 \quad (1)$$

where $\tilde{\Delta}_{n'} = \frac{\Delta_{n'} \pi T_c}{|\omega_{n'}|}$, $a = \frac{\langle g_{\mathbf{k}}^* \lambda_{\mathbf{k}\mathbf{k}'} g_{\mathbf{k}'} \rangle_{\mathbf{k}, \mathbf{k}'}^{FS}}{\langle |g_{\mathbf{k}}|^2 \rangle_{\mathbf{k}}^{FS}}$, $b = \frac{\mu^* \langle |g_{\mathbf{k}'}|^2 \rangle_{\mathbf{k}'}^{FS}}{\langle |g_{\mathbf{k}}|^2 \rangle_{\mathbf{k}}^{FS}}$, $c = \frac{\langle \lambda_{\mathbf{k}} |g_{\mathbf{k}}|^2 \rangle_{\mathbf{k}}^{FS}}{\langle |g_{\mathbf{k}}|^2 \rangle_{\mathbf{k}}^{FS}}$, $\lambda_{\mathbf{k}} = \langle \lambda_{\mathbf{k}, \mathbf{k}'} \rangle_{\mathbf{k}, \mathbf{k}'}^{FS}$ and even frequency pairing is explicitly assumed. The Coulomb pseudopotential, μ^* , is taken as band independent. The T_c can be calculated by Eq.(1) provided that $g_{\mathbf{k}}$ is known. The latter can be obtained by the second eigenvalue equation:

$$Z_{\mathbf{k}}^{-1} \langle (\lambda_{\mathbf{k}, \mathbf{k}'} - \mu^*) g_{\mathbf{k}'} \rangle_{\mathbf{k}'}^{FS} = \rho g_{\mathbf{k}} \quad (2)$$

with $Z_{\mathbf{k}} = 1 + \lambda_{\mathbf{k}}$. Eq.(2), when solved *self-consistently*, yields the symmetry and the exact momentum dependence of the SC gap. This modelling, permits us to calculate accurately $g_{\mathbf{k}}$ with a large resolution of grid points and then obtain the exact T_c within the full Eliashberg framework. The linearized equations do not provide information on the SC gap below T_c , e.g. whether the SC symmetry changes with T. In order to estimate such a possibility, we also calculate $g_{\mathbf{k}}$ at $T=0$ using the BCS-like self-consistent equation:

$$\Delta_{\mathbf{k}} = Z_{\mathbf{k}}^{-1} \langle (\lambda_{\mathbf{k}, \mathbf{k}'} - \mu^*) \Delta_{\mathbf{k}'} \sinh^{-1}(\omega_D / |\Delta_{\mathbf{k}'}|) \rangle_{\mathbf{k}'}^{FS} \quad (3)$$

where ω_D is the Debye frequency. The above, supplemented with the respective free energy formula, provides an approximate description for the gap structure at $T=0$ in the limit where the feedback of the gap on the renormalization function is negligible (for details see the SOM). Using the solution of Eq.(S16) in Eq.(1), we can calculate the anticipated T_c of the $T=0$ state. A combination of the $T=0$ and $T=T_c$ results suffices in order

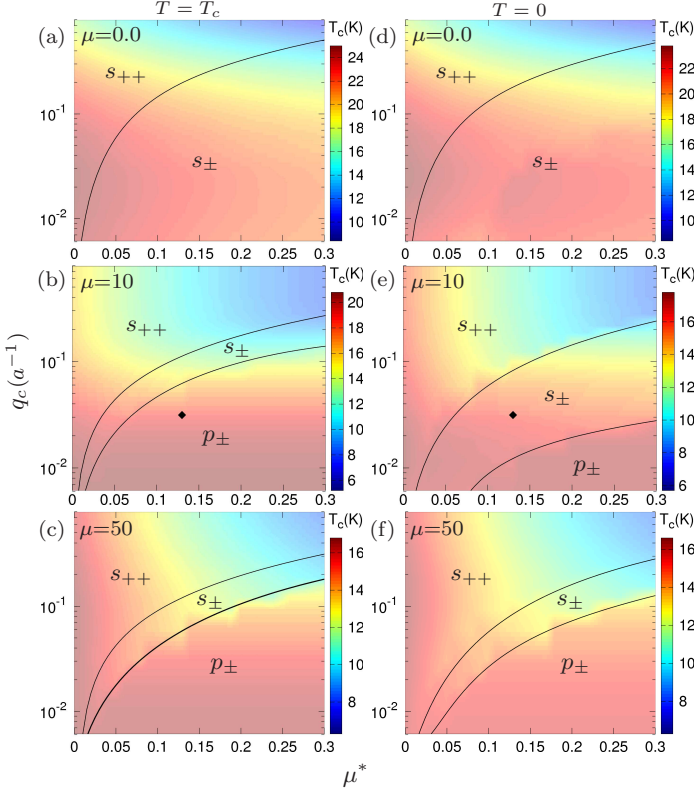


FIG. 2. (Color online) (a)-(c) Self-consistently calculated phase diagrams as a function of the Coulomb pseudopotential μ^* and the EPI momentum cut-off q_c , for $\lambda=1.38$ and $\mu=[0, 10, 50]$ meV at $T=T_c$. The y-axis is logarithmic to highlight the small- q_c region. The background color grade corresponds to the calculated T_c at each (q_c, μ^*) value. (d)-(f) Same plots at $T=0$. Here, the color grade is for calculations of the *anticipated* T_c from the low-T momentum structure of the SC gap, as described in the text. The notation s_{++} , s_{\pm} and p_{\pm} is for anisotropic one-sign and extended sign-alternating singlet s -wave and chiral triplet SC gap symmetries, respectively. It is easy to observe that the $\mu=0$ and $\mu=50$ meV results for both T limits agree very well with each other. Hence, at these doping levels, we expect that the symmetry of the SC gap found for $T = T_c$ is unchanged down to zero T. On the contrary, for intermediate dopings (here $\mu=10$ meV), there is a large parameter regime where the low-T gap symmetry is singlet s_{\pm} , while for higher temperatures, we find chiral triplet SC (e.g. compare the situation marked by the diamond symbols in Fig.(b) and (e)). These findings are in perfect agreement with the recently observed singlet to triplet SC temperature induced transitions in LiFeAs [11] (see Fig.4 for $H=0$).

to discern possible changes in the SC symmetry with T. We solve Eq.(2) *self-consistently* over a 512×512 grid of k -points for various initial forms of $g_{\mathbf{k}}$ including every allowed symmetry of the D_{4h} group or random values. The solution that is kept, maximizes the eigenvalue ρ . Next, the coefficients a, b, c are calculated and plugged into Eq.(1) which is solved for the T_c . The cutoff frequency used is $\omega_c = 10\omega_D$, where for ω_D we use the

calculated logarithmic frequency $\omega_{ln}=100$ K [37]. These steps are repeated varying $\mu \in [0, 50 \text{ meV}]$, $q_c \in [\frac{\pi}{512a}, \frac{\pi}{4a}]$ (the lattice constant $a=1$) and $\mu^* \in [0, 0.3]$ while keeping $\lambda=1.38$ fixed. The same procedure is followed for Eq.(S16) where the correct solution minimizes the free energy.

The obtained q_c - μ^* phase diagrams (PD) and the calculated T_c for various dopings at $T=T_c$ are shown in Fig.2(a)-(c). In the stoichiometric regime (Fig.2(a)), singlet A_{1g} states dominate the PD. This behavior can be attributed to the respective FS topology of LiFeAs shown in Fig.1(a). Due to the VHp at Γ , electrons from the isotropic α -band have a pronounced contribution to SC pairing thus favoring isotropic gap structures over SC symmetries with nodes such as d or p-wave. For relatively large q_c values, we find a one-sign anisotropic, s_{++} , SC gap. Decreasing q_c or increasing μ^* the system, in order to avoid the pair-breaking Coulomb repulsion, enters into a sign-alternating nodeless s_{\pm} state. Even in the latter, the symmetry is not pure s_{\pm} , but a strong s-wave component is superimposed. Hence, the T_c of both states is affected by μ^* , since $b \neq 0$ in Eq.(1). Notice how T_c increases with decreasing q_c since then, the EPC becomes sharply peaked and tends to become purely intraband, maximizing the contribution to SC pairing.

From the T_c dependence, it can be seen that there is a reasonable parameter space where our phononic theory produces the experimental $T_c \approx 18$ K of LiFeAs. For this parameter space ($q_c > 0.1$) we find that in both s_{++} and s_{\pm} regimes the gap over the α -pocket is the largest and isotropic. This is a result of the combined VHp and MD effects. The gap on the other FS sheets shows anisotropy that varies depending on symmetry. In the s_{\pm} state, the β -pocket exhibits maxima along the Γ -X and the electron pockets along the X-M direction, respectively. In the s_{++} state, the β -pocket exhibits maxima along the Γ -X and the electron pockets along the Γ -M direction. The latter features match precisely the T_c dependence reported by ARPES for this material [6, 7]. For example, for $\mu^* = 0.13$ and $q_c = 0.25$ we find s_{++} SC with $T_c \approx 18$ K and FS momentum dependence as shown in Fig.3(b).

In the non-stoichiometric case the α -pocket is removed from the FS as can be seen in Fig.1(b)-(c) for $\mu = 10$ and $\mu = 50$ meV, respectively. The remaining anisotropic FS possesses minima along the directions parallel and perpendicular to Γ -X that are enhanced with μ . Hence, the system tends to allow nodes or gap minima in these directions, possibly favoring d_{xy} or p-wave SC. The respective $T=T_c$ PDs are shown in Fig.2(b)-(c). Increasing μ^* the s_{\pm} region shrinks and at $q_c \lesssim 0.1$, a *p-wave SC state* ($g_{\mathbf{k}} \sim \sin k_x$ or $\sin k_y$) is indeed stabilized. Since in our formalism SC pairing is intraband, this is necessary spin triplet in order for the antisymmetry of the electron wavefunction to be satisfied. Free energy calculations at $T=0$, indicate that the stable solution is in fact *chiral* ($g_{\mathbf{k}} \sim \sin k_x \pm i \sin k_y$), which we hereafter

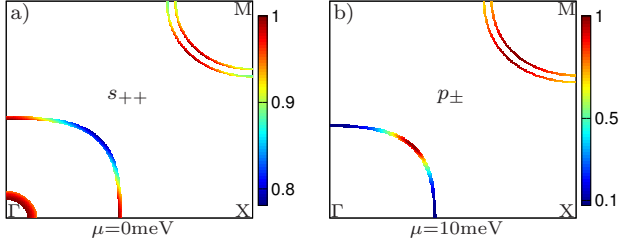


FIG. 3. (Color online) Self-consistently obtained momentum dependence of the SC gap ($|g_{\mathbf{k}}|$) at $T=T_c$ for $\lambda=1.38$ and $\mu^*=0.13$ in the (a) stoichiometric s_{++} regime ($\mu=0\text{meV}$, $q_c=0.25$) and (b) in the non-stoichiometric p_{\pm} regime ($\mu=10\text{meV}$, $q_c=0.032$). The gap on each band is normalized to unity in order to highlight the location of gap minima/maxima. The s_{++} SC gap in (a) has the exact FS momentum dependence reported by ARPES [6, 7].

refer to as p_{\pm} . The absence of the VHp affects also the T_c which gradually decreases with μ . For small μ , this decrease can be compensated with a decrease in q_c , as is evident in Fig.2(b). Remarkably, for (q_c, μ^*) values that yield $T_c \approx 18\text{K}$, the system is in the p_{\pm} state. The occurrence of p_{\pm} SC *only* for $\mu > 0$ within our theory is in perfect agreement with QPI [8] and particularly NMR [9, 11] reports, where in the latter it has been explicitly associated with non-stoichiometry. Moreover, it resolves the conflict between the reported triplet SC and ARPES data that indicate a strong EPI in LiFeAs [15].

We now compare our $T=0$ results with the ones at $T=T_c$. The $T=0$ PDs for $\mu=[0, 10, 50]\text{meV}$ are shown in Fig.2(d)-(f). For $\mu=0$ (Fig.2(a) and (d)), it is easy to notice that not only the PDs but also the calculated T_c 's, in the parameter region of interest discussed above, agree nicely. The same also holds for the $\mu=50\text{meV}$ results (Fig.2(c) and (f)). In fact, for $\mu > 50\text{meV}$, the two PD's become exactly the same. Hence, we conclude that the $T=0$ approximation works very well both in determining the PD as well as predicting the T_c . On this firm basis we estimate that for $\mu=0$ ($\mu \geq 50\text{meV}$) LiFeAs is in a s_{++} (p_{\pm}) state down to zero T .

Our solutions for $0 < \mu < 50\text{meV}$ are amenable to an interesting interpretation. In this regime, we systematically find that for relevant (q_c, μ^*) values, the SC symmetry at $T=0$ is s_{\pm} , while at $T=T_c$ it is p_{\pm} . Moreover, the expected T_c for the s_{\pm} is smaller than the T_c of the p_{\pm} state. Thus, we find clear evidence of a *temperature induced transition from singlet s_{\pm} to triplet p_{\pm} SC that can take place for small deviations from stoichiometry in LiFeAs*. Remarkably, such transitions have been reported very recently by NMR in samples that are slightly non-stoichiometric [11]. For example, for $\mu=10\text{meV}$, $\mu^*=0.13$ and $q_c=0.032$, we find two successive transitions, to p_{\pm} SC below $T_{c1} \approx 18\text{K}$ and to s_{\pm} SC below $T_{c2} \approx 16\text{K}$ (see diamond symbol in Fig.2(b) and (e)), in perfect agreement with the findings of the latter experiments summarized in Fig.4 of ref.[11]. Due to the

TABLE I. Summary of key results for $\lambda=1.38$, $\mu^*=0.13$

μ (meV)	q_c	T_{c1} (K)	$g_1(\mathbf{k})$	T_{c2} (K)	$g_2(\mathbf{k})$
0	0.25	18.2	s_{++}	-	-
10	0.042	18	p_{\pm}	15.6	s_{\pm}
50	0.032	15.5	p_{\pm}	-	-

small- q_c values in this region, the enhanced MD leads to a SC gap structure whose FS momentum dependence follows closely the FS DOS. Thus, we predict that the SC gap in both the s_{\pm} and p_{\pm} regions should exhibit maxima along Γ -M, as is shown e.g. in Fig.3(c). Our key results for $\mu^*=0.13$ are summarized on Table I.

Finally, given the close proximity of s_{++} , s_{\pm} and p_{\pm} states found within our theory, it is natural to expect that an applied magnetic field would induce a singlet to triplet transition in LiFeAs, either by suppressing singlet pairing or by enhancing the FS DOS anisotropy or both, thus favoring p_{\pm} SC. Hence, our mechanism could provide a plausible explanation for the experimental reports of a field induced triplet SC phase in this material [9–11].

In conclusion, we have presented a theory from the small- q phonon perspective, within which a plethora of controversial and yet unexplained experimental findings in SC LiFeAs are coherently understood. Based on realistic, fully anisotropic Eliashberg calculations, we have demonstrated how the interplay of this small- q EPI and the intrinsic FS properties of LiFeAs, governed by the presence of a VHp at the center of the BZ, result in a delicate balance between singlet s_{++}, s_{\pm} and triplet chiral $p_x + ip_y$ SC. Furthermore, we explicitly showed that slight deviations from stoichiometry and/or changes in temperature may favor one of these states. Our results resolve the conflict between a strong EPC and one sign singlet SC reported by ARPES and unconventional and, most interestingly, chiral triplet SC observed by other probes. In addition, they provide a systematic understanding for the occurrence of triplet SC in non stoichiometric samples as well as the temperature induced singlet to triplet SC transitions reported very recently. The accuracy of the present results and the exotic character of the involved SC states, establish that the small- q EPI mechanism should be considered on an *equal footing* with spin and other purely electronic mechanisms, in the analysis of *any* unconventional superconductor. Clearly, even the most exotic SC states like the chiral spin triplet reported here, should not exclude apriori our phononic mechanism.

We are grateful to S.Borisenko and B.Büchner for enlightening discussions. We also thank S.Borisenko for providing us the ARPES TB fit for LiFeAs prior to its publication. A.A. acknowledges financial support by IIEBE of National Technical University of Athens.

-
- * aaperis@mail.ntua.gr
† varelogi@mail.ntua.gr
- [1] M.J. Pitcher *et al.*, Chem. Commun. **45**, 5918 (2008); J.H. Tapp *et al.*, Phys. Rev. B **78**, 060505 (2008); X.C. Wang *et al.*, Solid State Commun. **148**, 538 (2008).
[2] Z. Li *et al.*, J. Phys. Soc. Jpn. **79**, 083702 (2010).
[3] A.E. Taylor *et al.*, Phys. Rev. B **83**, 220514(R) (2011).
[4] D.-J. Jang *et al.*, Phys. Rev. B **85**, 180505(R) (2012).
[5] I.I. Mazin and J. Schmalian, Physica C **469**, 614 (2009).
[6] S.V. Borisenko *et al.*, Symmetry **4**, 251 (2012).
[7] K. Umezawa *et al.*, Phys. Rev. Lett. **108**, 037002 (2012).
[8] T. Hänke *et al.*, Phys. Rev. Lett. **108**, 127001 (2012).
[9] S.-H. Baek *et al.*, Eur. Phys. J. B **85**, 159 (2012).
[10] G. Li *et al.*, Phys. Rev. B **87**, 024512 (2013).
[11] S.-H. Baek *et al.*, arXiv:1211.1594.
[12] S.V. Borisenko *et al.*, Phys. Rev. Lett. **105**, 067002 (2010).
[13] N. Qureshi *et al.*, Phys. Rev. Lett. **108**, 117001 (2012).
[14] J. Knolle *et al.*, Phys. Rev. B **86**, 174519 (2012).
[15] A. A. Kordyuk *et al.*, Phys. Rev. B **83**, 134513 (2011).
[16] P.M.R. Brydon *et al.*, Phys. Rev. B **83**, 060501(R) (2011).
[17] H. Kontani and S. Onari, Phys. Rev. Lett. **104**, 157001 (2010).
[18] S. Johnston *et al.*, Phys. Rev. Lett. **108**, 166404 (2012).
[19] H. Krackauer, W. Pickett and R.E. Cohen, Phys. Rev. B **47**, 1002 (1993).
[20] A. A. Abrikosov, Physica C **222**, 191 (1994); Phys. Rev. B **51**, 11955 (1995).
[21] M. Weger *et al.*, J. Low Temp. Phys. **95**, 131 (1994); M. Weger and M. Peter, Physica C **317-318**, 252 (1999).
[22] M. L. Kulić and R. Zeyher, Phys. Rev. B **49**, 4395 (1994).
[23] M. Grilli and C. Castellani, Phys. Rev. B **50**, 16880 (1994).
[24] G. Varelogiannis *et al.*, Phys. Rev. B **54**, R6877 (1996).
[25] G. Varelogiannis, Phys. Rev. B **57**, 13743 (1998).
[26] Z.B. Huang *et al.*, Phys. Rev. B **68**, 220507(R) (2003).
[27] S. Johnston *et al.*, Phys. Rev. B **82**, 064513 (2010).
[28] G.A. Sawatzky *et al.*, EPL **86**, 17006 (2009); M.L. Kulić and A.A. Haghighirad EPL **87**, 17007 (2009).
[29] S.L. Drechsler *et al.*, Physica C **470**, 332 (2010).
[30] G. Varelogiannis, Phys. Rev. Lett. **88**, 117005 (2002); Y. Suginishi and H. Shimahara, J. Phys. Soc. Jpn. **73**, 3121 (2004).
[31] P.M. Oppeneer and G. Varelogiannis, Phys. Rev. B **68**, 214512 (2003).
[32] X.-S. Ye, Z.-J. Yao and J.-X. Li, J. Phys. Condens. Matter **20**, 045227 (2008).
[33] A. Aperis *et al.*, Phys. Rev. B **83**, 092505 (2011).
[34] R.H. Liu *et al.*, Nature **459**, 64 (2009); R. Khasanov *et al.*, New J. Phys. **12**, 073024 (2010).
[35] A. Lankau *et al.*, Phys. Rev. B **82**, 184518 (2010).
[36] H.J. Choi *et al.*, Nature **418**, 758 (2002).
[37] R.A. Jishi and H.M. Alyahyaei, Adv. Condens.Matter Phys. **2010**, 804343 (2010).
-

Supplementary Online Material for “Phonon mediated singlet and chiral spin triplet superconductivity in LiFeAs”

SMALL-Q ELECTRON-PHONON COUPLING AND ITS SEPARABILITY

In this section, we discuss the simplest situation when a small-q electron-phonon coupling (EPC) may arise and show how the obtained EPC maps to a separable one without affecting any of the basic physics. The EPC function is defined as:

$$\lambda(\mathbf{k}, \mathbf{k}'; n, n') = 2 \int_0^\infty \frac{\alpha^2 F(\mathbf{k}, \mathbf{k}'; \Omega) \Omega}{(\omega_n - \omega_{n'})^2 + \Omega^2} d\Omega \quad (\text{S1})$$

where $\alpha^2 F(\mathbf{k}, \mathbf{k}'; \Omega)$ is the momentum dependent electron-phonon spectral function (EPSF), which for a single phonon branch is:

$$\alpha^2 F(\mathbf{k}, \mathbf{k}'; \Omega) = N_0 |g_{\mathbf{k}\mathbf{k}'}|^2 \delta(\Omega - \omega_{\mathbf{k}-\mathbf{k}'}) \quad (\text{S2})$$

with $g_{\mathbf{k}\mathbf{k}'}$ the electron-phonon matrix element (EPME) [1]. Perhaps the most common situation when small-q processes dominate can take place when large dielectricity and the long range nature of the Coulomb potential are considered, as first discussed by Abrikosov (ref. [20] of main text). As a paradigm, we analyze this case in some detail. Due to the modulation of the screened Coulomb potential, there exists a first-order coupling between electrons and phonons [2]. In this case, the electron-phonon matrix element is given by:

$$g_{\mathbf{q}} = \sqrt{\frac{\hbar}{2M\omega_{\mathbf{q}}}} \hat{\epsilon}_{\mathbf{q}} \cdot \mathbf{q} \frac{V_{\mathbf{q}}}{\epsilon_{\mathbf{q}}} \quad (\text{S3})$$

where $\mathbf{q} = \mathbf{k} - \mathbf{k}'$ is the exchanged momentum, M is the ionic mass, $\omega_{\mathbf{q}}$ is the renormalized phonon dispersion, $\hat{\epsilon}_{\mathbf{q}}$ is the phonon polarization, $V_{\mathbf{q}} = \frac{4\pi e^2}{\epsilon q^2}$ is the bare Coulomb potential, ϵ is the static dielectric constant and $\epsilon_{\mathbf{q}}$ is the static dielectric function. The renormalized phonon dispersion is just $\omega_{\mathbf{q}} = \frac{\Omega_p}{\sqrt{\epsilon_{\mathbf{q}}}}$, where Ω_p is the phonon plasma frequency. In the simplest picture, the dielectric function can be written in the Thomas-Fermi approximation as: $\epsilon_{\mathbf{q}} = 1 + \frac{q_{TF}^2}{q^2}$, where q_{TF} is the Thomas-Fermi screening wavevector and $q_{TF} = \sqrt{4\pi e^2 N_0 / \epsilon}$.

Compining the above relations, the EPC can be written in the following form:

$$\lambda(\mathbf{q}; m) = N_0 V_{ep} \frac{1}{q^2 + q_{TF}^2} \frac{\frac{q^2 \Omega_p^2}{q^2 + q_{TF}^2}}{w_m^2 + \frac{q^2 \Omega_p^2}{q^2 + q_{TF}^2}} \quad (S4)$$

where the effective parameter V_{ep} includes all remaining terms and $w_m = 2m\pi T$ is a bosonic frequency ($m = n - n'$). The EPC has a small- q momentum dependence peaked at $q = q_{TF}$ and a Lorentzian frequency dependence whose width is determined again by q_{TF} . Thus, even in this rough approximation, the EPC acquires a small- q momentum dependence with the momentum cutoff defined by the Thomas-Fermi screening wavevector. The peak at small- q gets more pronounced by reduction of the density of states or an increase in the dielectric constant. At low energies, ($w=0$ or $T=0$), Eq.(S4) reduces to:

$$\lambda(\mathbf{q}) = N_0 V_{ep} \frac{1}{q^2 + q_{TF}^2} \quad (S5)$$

Increasing the ratio T/Ω_p , Eq.(S4) approaches the form of Eq.(S5) for $m \neq 0$. For parameters relevant to LiFeAs this is the case near $T \approx T_c$ (i.e. see Fig.S1). Thus, $\lambda_{\mathbf{q},m}$ behaves like a separable function over momentum and frequency in the physical range that we are interested in.

Separable small-q EPC

Let us now assume an effective separable EPC. This can be achieved, for example, if the EPSF is separable and the frequency dependent part is described by an Einstein spectrum [3, 4]:

$$\alpha_E^2 F(\mathbf{k}, \mathbf{k}'; \Omega) = \lambda_{\mathbf{k}\mathbf{k}'} \frac{\Omega_E}{2} \delta(\Omega - \Omega_E) \quad (S6)$$

Inserting Eq.(S6) into Eq.(S1) one easily gets:

$$\lambda(\mathbf{k}, \mathbf{k}'; n, n') = \lambda_{\mathbf{k}\mathbf{k}'} \frac{\Omega_E^2}{(\omega_n - \omega_{n'})^2 + \Omega_E^2} = \lambda_{\mathbf{k}\mathbf{k}'} \lambda_{nn'} \quad (S7)$$

At low energies ($n = n' / T=0$) the above reduces to: $\lambda_{\mathbf{k}\mathbf{k}'}$ which we assume to have a small- q structure within a cutoff q_c . Thus, we can write:

$$\lambda_{sep}(\mathbf{q}; m) = N_0 V_{ep} \frac{1}{q^2 + q_c^2} \frac{\Omega_E^2}{w_m^2 + \Omega_E^2} \quad (S8)$$

Obviously, the above matches exactly Eq.(S4) at low energies ($w=0/T=0$) and for $q_c = q_{TF}$, $\Omega_p = \Omega_E$. In our calculations for LiFeAs, we set $\Omega_{p(E)} = \omega_{log} = 100$ K (ref. [37] of main text). We observe that already at $T=10$ K the EPC of Eq.(S1) and Eq.(S8) agree very well as it is shown in Fig.S1.

MULTIBAND MOMENTUM DEPENDENT ELIASHBERG FORMALISM

Our starting point is the system of coupled anisotropic Eliashberg equations at the finite temperature:

$$Z_{\mathbf{k},n} = 1 + \frac{\pi T}{\omega_n} \sum_{n'} \langle \lambda(\mathbf{k}, \mathbf{k}'; n, n') \frac{\omega_{n'}}{\sqrt{\omega_{n'}^2 + \Delta_{\mathbf{k}',n'}^2}} \rangle_{\mathbf{k}'}^{FS} \quad (S9)$$

$$Z_{\mathbf{k},n} \Delta_{\mathbf{k},n} = \pi T \sum_{n'}^{| \omega_{n'} | < \omega_c} \langle \left[\lambda(\mathbf{k}, \mathbf{k}'; n, n') - \mu^*(\omega_c) \right] \frac{\Delta_{\mathbf{k}',n'}}{\sqrt{\omega_{n'}^2 + \Delta_{\mathbf{k}',n'}^2}} \rangle_{\mathbf{k}'}^{FS} \quad (S10)$$

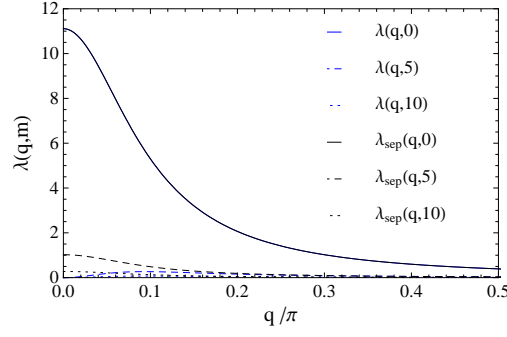


FIG. S1. Momentum dependence of $\lambda(\mathbf{q}, m)$, $\lambda_{sep}(\mathbf{q}, m)$ for $q_{TF(c)}=0.3$, $\Omega_{p(E)}=100\text{K}$ at $T=10\text{K}$ and different Matsubara frequencies. The agreement between λ and λ_{sep} is evident.

where the n th Matsubara frequency $\omega_n = (2n + 1)\pi T$, $Z_{\mathbf{k},n} = Z(\mathbf{k}, i\omega_n)$ is the strong-coupling renormalization parameter, $\Delta_{\mathbf{k},n} = \Delta(\mathbf{k}, i\omega_n)$ is the SC gap function, $\lambda(\mathbf{k}, \mathbf{k}'; n, n')$ the EPC and $\mu^*(\omega_c)$ is the Coulomb pseudopotential which comes with a cutoff ω_c in the Matsubara frequency summation and is taken as band independent. The notation $\langle \dots \rangle_{\mathbf{k}}^{FS} = \sum_{\mathbf{k}} \frac{N_{\mathbf{k}}}{N_0} (\dots)$ means an average over the entire FS, where N_0 is the Density of States (DOS), $N_{\mathbf{k}} = |\nabla \xi_{\mathbf{k}F}|^{-1}$ the angularly resolved DOS (arDOS) and $\xi_{\mathbf{k}}$ the energy dispersion at the Fermi level ($\sum_{\mathbf{k} \in FS} \frac{N_{\mathbf{k}}}{N_0} = 1$). In this formalism, all band structure effects are conveniently encoded in the FS averages and the anisotropy of the FS is fully taken into account.

Eq.(S9)-(S10) provide the strong coupling description of a phonon mediated, singlet or unitary triplet, superconductor (e.g. see [5]) having an arbitrary number of bands contributing to the FS [6]. In this sense, $\Delta_{\mathbf{k},n}$, $Z_{\mathbf{k},n}$ are global quantities defined over the entire FS. For an i -band SC, it is possible to degrade the above into a system of $2i$ -coupled equations for $\Delta_{\mathbf{k},n}^i$, $Z_{\mathbf{k},n}^i$ defined on each separate band, however by doing so, the momentum dependence of the EPC is lost (e.g. see ref.[6]). Thus, throughout this study, we work in the most generalized framework as defined above. Note that, since the values of μ that we consider are very small, we have neglected the energy shift self-energy term.

Equations at T_c in the separable model

Linearizing the above system at T_c , introducing the separable approximation: $\lambda(\mathbf{k}, \mathbf{k}'; n, n') = \lambda_{\mathbf{k},\mathbf{k}'} \lambda_{n,n'}$ and re-expressing the Matsubara sum on positive frequencies yields:

$$Z_{\mathbf{k},n} = 1 + \lambda_{\mathbf{k}} \frac{1}{2n+1} \left(\lambda(0) + 2 \sum_{m=1}^n \lambda(m) \right) \quad (\text{S11})$$

$$Z_{\mathbf{k},n} \Delta_{\mathbf{k},n} = \sum_{n'=0}^{\omega_{n'} < \omega_c} w_{n'} \left\{ \lambda_{\mathbf{k},\mathbf{k}'} (\lambda_{n-n'} + \lambda_{n+n'+1}) - 2\mu^*(\omega_c) \right\} \Delta_{\mathbf{k}',n'} \rangle_{\mathbf{k}'}^{FS} \quad (\text{S12})$$

where we have explicitly assumed even frequency SC and $\lambda_{\mathbf{k}} = \langle \lambda_{\mathbf{k},\mathbf{k}'} \rangle_{\mathbf{k}'}^{FS}$, $w_n = \frac{1}{2n+1}$, and we have used the relation: $\sum_{n'} \lambda_{nn'} \frac{\omega_{n'}}{|\omega_{n'}|} = \lambda(0) + 2 \sum_{m=1}^n \lambda(m)$. From Eq.(S11), it is evident that $Z_{\mathbf{k},n}$ has become separable. Inserting Eq.(S11) into Eq.(S12) we see that the SC gap has also acquired a separable structure and thus, we can write: $\Delta_{\mathbf{k},n} = \Delta_n g_{\mathbf{k}}$, where Δ_n contains the frequency and $|g_{\mathbf{k}}| \leq 1$ the momentum dependence, respectively.

Inserting Eq.(S11) into Eq.(S12), multiplying both sides with $g_{\mathbf{k}}^i = \frac{g_{\mathbf{k}}^i}{\langle |g_{\mathbf{k}}|^2 \rangle_{\mathbf{k}}^{FS}}$ and then taking the FS average gives:

$$\Delta_n = \sum_{n'=0}^{\omega_{n'} < \omega_c} \left[\left\{ \frac{\langle g_{\mathbf{k}}^* \lambda_{\mathbf{k},\mathbf{k}'} g_{\mathbf{k}'} \rangle_{\mathbf{k},\mathbf{k}'}^{FS}}{\langle |g_{\mathbf{k}}|^2 \rangle_{\mathbf{k}}^{FS}} (\lambda_{n-n'} + \lambda_{n+n'+1}) - 2\mu^*(\omega_c) \frac{\langle |g_{\mathbf{k}'}|^2 \rangle_{\mathbf{k}'}^{FS}}{\langle |g_{\mathbf{k}}|^2 \rangle_{\mathbf{k}}^{FS}} \right\} - \frac{\langle |g_{\mathbf{k}}|^2 \lambda_{\mathbf{k}} \rangle_{\mathbf{k}}^{FS}}{\langle |g_{\mathbf{k}}|^2 \rangle_{\mathbf{k}}^{FS}} \delta_{nn'} \right. \\ \left. \times \left(\lambda(0) + 2 \sum_{m=1}^{n'} \lambda(m) \right) \right] w_{n'} \Delta_{n'} \quad (\text{S13})$$

which, after some rearranging can be written as:

$$\sum_{n'=0}^N \left[a \cdot (\lambda(n - n') + \lambda(n + n' + 1)) - 2b - c \cdot \delta_{nn'} \times \left(\lambda(0) + 2 \sum_{m=1}^n \lambda(m) \right) - \frac{\delta_{nn'}}{w_{n'}} \right] \tilde{\Delta}_{n'} = 0$$

with $\tilde{\Delta}_{n'} = \Delta_{n'} w_{n'}$, $a = \frac{\langle g_{\mathbf{k}}^* \lambda_{\mathbf{k}\mathbf{k}'} g_{\mathbf{k}'} \rangle_{\mathbf{k}\mathbf{k}'}^{FS}}{\langle |g_{\mathbf{k}}|^2 \rangle_{\mathbf{k}}^{FS}}$, $b = \frac{\mu^* \langle g_{\mathbf{k}'} \rangle_{\mathbf{k}'}^{FS}}{\langle |g_{\mathbf{k}}|^2 \rangle_{\mathbf{k}}^{FS}}$ and $c = \frac{\langle \lambda_{\mathbf{k}} | g_{\mathbf{k}} |^2 \rangle_{\mathbf{k}}^{FS}}{\langle |g_{\mathbf{k}}|^2 \rangle_{\mathbf{k}}^{FS}}$. The above is an eigenvalue problem similar to the one encountered in usual Eliashberg theory [7] but extended to include the full momentum dependence of the SC gap and it can be solved following standard methods [5] for the T_c provided that $g_{\mathbf{k}}$ is known. Obviously, for $g_{\mathbf{k}} = 1$ the usual isotropic Eliashberg equation is retrieved.

Since $\Delta_{\mathbf{k},n} = \Delta_n g_{\mathbf{k}}$, we can apply a square-well ansatz [8] to Eq.(S11)-(S12) in order to extract an equation for the momentum dependent part of the SC gap:

$$\lambda(\mathbf{k}, \mathbf{k}'; n, n') = \begin{cases} \lambda_{\mathbf{k}, \mathbf{k}'} & \text{for both } |\omega_n|, |\omega_{n'}| < \omega_c, \\ 0 & \text{otherwise} \end{cases} \quad \text{and} \quad \Delta_n g_{\mathbf{k}} = \begin{cases} \Delta(T) g_{\mathbf{k}} & , \quad |\omega_n| < \omega_c, \\ 0 & , \quad |\omega_n| > \omega_c \end{cases}$$

It is easy to observe that within this model $Z_{\mathbf{k},n}$ becomes:

$$Z_{\mathbf{k}} = 1 + \lambda_{\mathbf{k}} \quad (\text{S14})$$

and the gap equation takes the form:

$$Z_{\mathbf{k}} g_{\mathbf{k}} \Delta(T) = \sum_{n'=0}^{|\omega_{n'}| < \omega_c} w_{n'} \langle \{2\lambda_{\mathbf{k}, \mathbf{k}'} - 2\mu^*(\omega_c)\} g_{\mathbf{k}'} \rangle_{\mathbf{k}'}^{FS} \Delta(T)$$

which after a standard summation on Matsubara frequencies yields:

$$Z_{\mathbf{k}}^{-1} \langle (\lambda_{\mathbf{k}, \mathbf{k}'} - \mu^*) g_{\mathbf{k}'} \rangle_{\mathbf{k}'}^{FS} = \rho g_{\mathbf{k}} \quad (\text{S15})$$

where $\rho^{-1} = \ln \left[\frac{1.13\omega_c}{T_c} \right]$. This is an eigenvalue equation for the momentum part of the SC gap alone, which when solved self-consistently provides the exact $g_{\mathbf{k}}$. Notice that in this case $g_{\mathbf{k}}$ is not just a form factor corresponding to an irreducible representation, but it is rather a superposition of form factors and all their harmonics of all the allowed irreducible representations, i.e. it is the *realistic* SC structure favored by the system's specific characteristics.

Equations at $T=0$ in the separable model

At $T=0$, the Eliashberg equations can be treated approximately to give a closed form, BCS-like equation. This can be achieved by neglecting $\Delta_{\mathbf{k},n}$ in Eq.(S9) and further applying the square-well ansatz (see e.g. ref.[9, 10]). Using $Z_{\mathbf{k}} = 1 + \lambda_{\mathbf{k}}$ in Eq.(S10) and taking the zero T limit ($T \sum_{n'} \rightarrow 2 \int_0^{\omega_c} \frac{d\omega}{2\pi}$) gives:

$$\Delta_{\mathbf{k}} = Z_{\mathbf{k}}^{-1} \langle (\lambda_{\mathbf{k}, \mathbf{k}'} - \mu^*) \Delta_{\mathbf{k}'} \sinh^{-1} \left(\frac{\omega_c}{|\Delta_{\mathbf{k}'}|} \right) \rangle_{\mathbf{k}'}^{FS} \quad (\text{S16})$$

After self-consistently solving the above equation, $g_{\mathbf{k}}$ is retrieved. The correct solution is determined by minimizing the respective free energy difference between the normal and the SC state within Eliashberg theory [11]. A momentum dependent expression for the latter is [12]:

$$\delta F = -\pi T N_0 \sum_n \langle \left(\sqrt{\omega_n^2 + \Delta_{\mathbf{k},n}^2} - |\omega_n| \right) \left(Z_{\mathbf{k},n} - Z_{\mathbf{k},n}^N \frac{|\omega_n|}{\sqrt{\omega_n^2 + \Delta_{\mathbf{k},n}^2}} \right) \rangle_{\mathbf{k}}^{FS}$$

Applying the square-well approximation, taking the $T=0$ integral over Matsubara frequencies and for $Z_{\mathbf{k}}^N = Z_{\mathbf{k}}$ we find the respective condensation energy as:

$$\delta F = N_0 \omega_c \langle Z_{\mathbf{k}} (\omega_c - \sqrt{\omega_c^2 + \Delta_{\mathbf{k}}^2}) \rangle_{\mathbf{k}}^{FS} \quad (\text{S17})$$

The isotropic version of Eq.(S16) has been previously considered in multiband Eliashberg theories, where it has been shown that it, in fact, captures the full Eliashberg results very well (e.g. see ref.[10]). Our results for LiFeAs,

indicate that this approximation scheme works also well, when the full momentum dependence is also included in the calculations.

* aaperis@mail.ntua.gr

† varelogi@mail.ntua.gr

- [1] G. Grimvall, *The Electron-Phonon Interaction in Metals* (North-Holland Publishing Co., Amsterdam), 1981.
 - [2] J.R. Schrieffer, *Theory of Superconductivity* (W.A. Benjamin, New York), 1964.
 - [3] M.Daams and J.P. Carbotte, J. Low Temp. Phys. **43**, 263 (1981);
 - [4] A. J. Millis, S. Sachdev and C. M. Varma, Phys. Rev. B **37**, 4975 (1988).
 - [5] P.B. Allen and B. Mitrović, Solid State Phys. **37** (1982).
 - [6] H.J. Choi, M.L. Cohen and S.G. Louie, Phys. Rev. B **73**, 104520 (2006).
 - [7] P.B. Allen and R.C. Dynes, Phys. Rev. B **12**, 905 (1975).
 - [8] J.P. Carbotte, Rev. Mod. Phys. **62**, 1027 (1990).
 - [9] E.J. Nicol and J.P. Carbotte, Phys. Rev. B **71**, 054501 (2005).
 - [10] O.V. Dolgov *et al.*, Phys. Rev. B **79**, 060502(R) (2009).
 - [11] J. Bardeen, M. Stephen, Phys. Rev. **136**, A1485 (1964).
 - [12] H.J. Choi, M.L. Cohen and S.G. Louie, Physica C **385**, 66 (2003).
-